

# AWFCNET: An Attention-Aware Deep Learning Network with Fusion Classifier for Breast Cancer Classification Using Enhanced Mammograms

Renato R. Maaliw III

*College of Engineering  
Southern Luzon State University  
Lucban, Quezon, Philippines  
rmaaliw@slsu.edu.ph*

Pitz Gerald G. Lagrazon  
*College of Engineering  
Southern Luzon State University  
Lucban, Quezon, Philippines  
pitzgerald.lagrazon@gmail.com*

Mukesh Soni

*Department of CSE  
Chandigarh University  
Mohali, Punjab, India  
mukesh.research24@gmail.com*

Mariebeth P. Seño  
*College of Arts & Sciences  
Southern Luzon State University  
Lucban, Quezon, Philippines  
mpseno@slsu.edu.ph*

Manuel P. Delos Santos

*College of Allied Medicine  
Southern Luzon State University  
Lucban, Quezon, Philippines  
mdelossantos@slsu.edu.ph*

Maria Rossana D. de Veluz

*College of Engineering  
Southern Luzon State University  
Lucban, Quezon, Philippines  
mrddveluz@slsu.edu.ph*

Reynaldo V. Danganan  
*College of Industrial Technology  
Southern Luzon State University  
Lucban, Quezon, Philippines  
rdanganan@slsu.edu.ph*

**Abstract**—Breast cancer remains a significant public health concern and a leading cause of female mortality despite recent advances in healthcare. Experts agree that its early prognosis is a key to survivability. In this research, we proposed a deep learning architecture code-named AWFCNET. It comprised multiple segments of preprocessing techniques (color shifting & image enhancement), feature learning based on ResNeXt-101 convolutional network as a backbone with transfer and attention-aware mechanisms, and fusion classifier composed of three recurrent neural networks. The generalization capability of the pipeline produced 98.10% accuracy on a mammogram dataset using 10-fold cross-validation. Computational benchmarks revealed that it surpassed existing state-of-the-art approaches with provisions of visual interpretability via gradient maps. Thus, our framework could complement physicians' expertise in rapid and dependable breast cancer diagnoses.

**Keywords**—ensemble prediction, hybrid model, image enhancement, medical diagnosis, ResNeXt-101, tumors

## I. INTRODUCTION

Breast cancer (BC) is a lethal disease caused by the immediate mutation of internal nucleolus cells in the breast. Recent statistical figure reports its prevalence in women, accounting for 26% of all cancer cases. In 2021, an estimated 2.5 million instances and 630,000 deaths transpired worldwide [1]. According to specialists, these mortality rates can be reduced by 80% through early detection, where they are still easily treatable. Mammography, ultrasound, magnetic resonance imaging (MRI), histopathology, and thermography are widely used to produce clear pictures of internal organs for medical diagnosis. Despite these innovations, manually interpreting images is time-consuming, stressful, and inconsistent [2]. Comparing benign (non-aggressive) and malignant (aggressive) tumors are complex, as the difference between dense and cancerous tissue is challenging to comprehend (Fig. 1). Integration of state-of-the-art technology with established practices is paramount to improving prognosis. The advent of artificial intelligence (AI) has marked a significant advancement in computer-assisted

diagnosis (CAD) in supporting expert decisions [3]. As algorithms evolve, detecting differences in BC images becomes possible. It ensures observational results' uniformity, hence increasing objectivity and decreasing subjectivity.

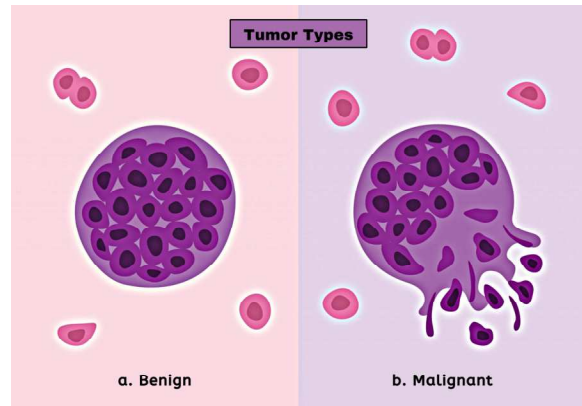


Fig. 1. Tumor types: a) benign (non-cancerous) and b) malignant (cancerous)

Over the past decades, scientists and professionals experimented with new breast mass preprocessing, segmentation, and classification methods using classical machine learning (ML). A study by [4] presented a mammogram tumor analysis utilizing a neural network (NN) for segmentation and recognition involving handcrafted features (HF). Researchers [5] applied K-nearest neighbors (KNN) and Naïve Bayes (NB) to discriminate between healthy and cancerous samples from clinical data, with KNN performing better. The works of [6] [7] leveraged distinct models with optimized hyperparameters using the Wisconsin dataset [8]. These included extreme machine learning (EML), artificial NN (ANN), support vector machines (SVM), KNN, and random forest (RF). Experts [9] processed a public mammogram dataset [10] using a Gabor wavelet transformation to construct image features with the help of decision trees (DT). Related studies of [11] yielded superior multi-layer perception (MLP) results than other methods in identifying BC. Proponent [12] developed a technique for

localized preservation of projections to decrease feature vector dimensionality in breast mammograms using bilateral asymmetry. It involved SVM and KNN for model testing, with a leave-one-out validation approach. To quantify morphological properties, [13] explored pairing variables learned on SVM and DT preprocessed using Fourier transformation, scale-invariant modification (SIM), and texture analysis. In an effort to speed up the process, [14] utilized region of interest (ROI) aimed at improving the ability to determine cancerous cells via Law's texture energy measurement with a discrimination rate of 93%. Although the outcomes of studies are promising, their performance is poor against deep learning (DL) architectures.

Recent cutting-edge DL procedures predicated on advanced CNNs showed significant improvements in BC classification efficiency. Authors [15] offered an alternative approach by creating a shallow (single) convolutional NN (CNN), but it had a limited capability to uncover latent patterns in image scans. Numerous scholars [16] [17] conducted the extraction of HF focused on categorizing malignant and benign specimens based on deep CNN (DCNN). Nonetheless, multiple studies [18 – 20] implied that HF attributes were inferior to automated DL features specifically in image recognition cases. Benchmarked results by [21] reinforced these findings on complex models of *ResNet50* (91%), *VGG-16* (94%), and *AlexNet* (95%) [22] using the Mammographic Image Analysis Society (MIAS) datasets. In contrast, article [23] made a lightweight CNN architecture to speed up the learning process. Nonetheless, it only achieved 83% precision because of oversimplification. Using ROI values, [24] preprocessed images and retrieved anomalous sections devoid of noise by applying Hough transformation to isolate breast mass (32 features) edges with 96% certainty.

Another approach used CNNs with an unsupervised EML to recognize lumps [25] according to texture, morphology, and density data with 86% accuracy. A firefly updated chicken based swarm optimization for tumor region identification on a hybrid classifier reported a three-classification (normal, benign & malignant) with a very satisfactory success rate [26]. Yet, its weakness resides in its procedural and computational overheads, as texture attributes were pre-identified rather than extracted from raw mammograms. Reference [27] fed patches of cropped photos into CNN with a categorization performance of 90% but its main drawback is that ROI hinged on external data. The investigation of [28] presented parasitic metric layers for binary classification, while [29] employed dynamic contrast-magnetic resonance imaging – both with very satisfactory reliability of 96% and 97%. They also recommended a localized tumor segmentation technique to derive the active contours based on breast MRIs to find the ROI intricately. Many studies have tried using augmented data to get better-generalized results. Simulations of [30] used a *ResNet50* and a marine predator's algorithm (MPA) to perform hybrid BC detection, increasing the sample size to 1290 images while maintaining 97% diagnostics accuracy. Similarly, [31] examined four benchmarked configuration of

CNNs using histogram equalization and principal component analysis to reduced features sizes on 1288 images. For the segmentation of 1028 images, researchers [32] implemented a U-Net network and evaluated five designs (*VGG16*, *ResNet50*, *MobileNetV2*, and *DenseNet21*), with *InceptionV3* proving to be the most practical. A multistage construction of NN and SVM (with three kernel functions) on 2576 mammograms attained a 97% prediction rate [33]. Scholars [34] proposed local binary pattern (LBP) and uniform manifold approximation and projection (UMAP) for feature extraction and reduction, respectively on synthetically enlarged data. It was trained on a 9-layer CNN framework.

Literature analysis reveals that CAD is progressing swiftly in BC detection, incorporating various preprocessing, segmentation, conventional, and advanced ML algorithms. Yes, we agree on the advantages of each stated method. However, we are optimistic that there are still unfilled gaps as AI can quickly convey cancer's finer details better than the naked eye, specifically in its early stages. To move the science forward, we proposed an automated pipeline anchored on attention-aware CNNs (A-ACNN) with a reinforcement learning mechanism and extensive preprocessing procedures. We also designed a fusion (ensemble) classifier at the architecture's tail-end to stabilize classification via majority voting to avoid under and overfitting for a more generalized output. Our study can help oncologists evaluate BC earlier to deliver timely patient treatments.

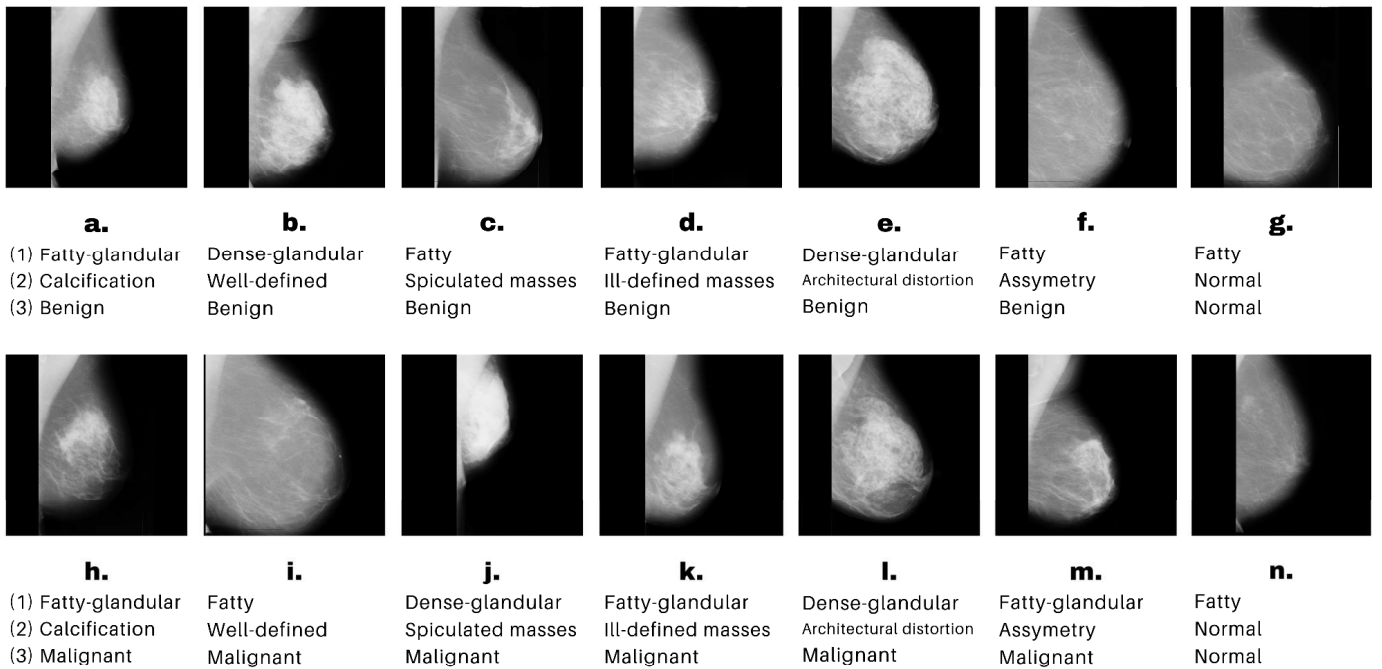
## II. METHODOLOGY

### A. Data Source

We compiled 322 high-resolution black-and-white mammography scans [22] subdivided into three distinct and equal categories. The original sample distributions were 64 (benign (B)), 51 (malignant (M)), and 207 (normal (N)). To manage the substantial inequality ratio of roughly 4:1 against N, we obtained additional related images from other sources [35] [36] to offset each category to the sample size of N (207). Assuring a balanced dataset was necessary for enhancing deep learning models' training, testing, and validation, as it removes bias towards a specific class. Furthermore, all images were resized to 1024 x 1024 pixels (px) to account for size discrepancies, then standardized to 512 x 512 px. Fig. 2 depicts a selection of samples annotated by medical professionals.

### B. Synthetic Data Enlargement and Balancing

Insufficient images impede improving pattern recognition as it dramatically impacts the machine learning model's performance. The main issues were rooted on the lack of comprehensive medical image samples available. Hence, augmentation was necessary to generate new synthetic data to increase variability to achieve training generalization and robustness. We performed a single transformation (horizontal flipping) to generate an additional 621 (207 x 3) images with a total of 1242, with 414 for each type (B, M & N). Finally, we partitioned the final dataset into 80% by 20% training and testing split with a 10-fold cross-validation.



**Notation:**

(1) Character of background tissue (2) Class of abnormality present, and (3) Severity of abnormality

Fig. 2. Excerpts of MIAS dataset showing mammogram images with benign (a to f), malignant (h to m), and normal (g & n) cases [22].

### C. Color Shifting and Image Enhancement

In image processing, color standardization is essential as it improves visual quality. It ensures increased interpretability by highlighting vital characteristics for maximum feature extraction while suppressing noise, making it easier for machine learning algorithms to examine and analyze images. We adjusted the optimized shifted colors using the following values: red = 0.19, green = 0.58 (prioritized) and blue = 0.23. Fig. 3 demonstrates the color channel comparisons for a malignant case.

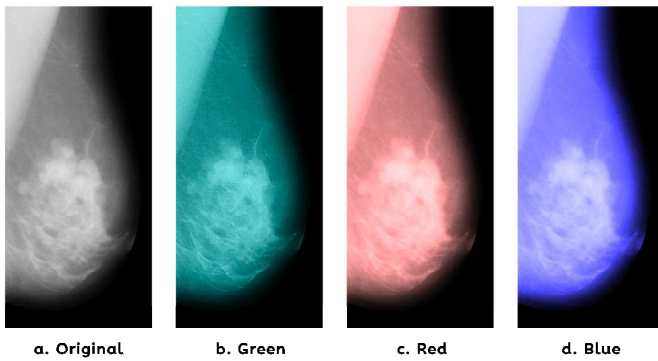


Fig. 3. Color shift comparison with reference to the original image (a), where the green channel provided extra details (b) than the others (c & d).

Benign and malignant breast cancer tissues are difficult to distinguish due to their resemblance in mammograms. They can appear as irregularly shaped masses that are crowded and proliferating rapidly. We conducted image enhancement procedures to solve this predicament since most samples had low contrasts resulting to insufficient details due to noise and blurring using a spatial Wiener filter (SWF) [35].

The process starts with an image  $o(x, y)$  with blurring or noise  $n(x, y)$  represented in Equation 1:

$$z(x, y) = o(x, y) + n(x, y) \quad (1)$$

where  $o(x, y)$  and  $z(x, y)$  is the original (OI) and noisy image (NI) correspondingly. The noise in its stationary form (presumably) is expressed with a mean of zero and variance  $\delta_n^2$  and uncorrelated with the OI modeled by Equation 2:

$$o(x, y) = m_s + w(x, y) \quad (2)$$

where  $m_s$  and  $\delta_s$  are neighboring (localized) mean and standard deviation (std). The  $w(x, y)$  indicates a zero mean noise of unit variance. SWF minimizes the mean square error (MSE) between the OI and the enhanced image (EI) of  $\hat{z}(x, y)$  derived from Equation 3:

$$\hat{z}(x, y) = \frac{s}{s^2 + r^2} o(x, y) - \frac{s}{s^2 + r^2} \quad (3)$$

$m_s$  and  $\delta_s$  are updated at each pixel and estimated from NI as expressed by Equations 4, 5, and 6:

$$\hat{n}_s(x, y) = \frac{1}{(2e+1)(2f+1)} \sum_{k=i-e}^{i+e} \sum_{l=-f}^{+f} v(k, l) \quad (4)$$

$$\delta^2(x, y) = \frac{1}{(2e+1)(2f+1)} \sum_{k=i-e}^{i+e} \sum_{l=-f}^{+f} v(k, l) - \hat{n}_s(x, y)^2 \quad (5)$$

$$\hat{\delta}_s(x, y) = \max\{0, \delta^2(x, y) - \delta_r^2\} \quad (6)$$

Then each update for  $\hat{m}_s(x, y)$  and  $\hat{\delta}_s(x, y)$  is substituted to Equation 3, becoming:

$$\hat{o}(x, y) = \hat{m}_s(x, y) + \frac{\hat{\delta}_s^2(x, y)}{\hat{\delta}_s^2(x, y) + \frac{r^2}{r}} [z(x, y) - \hat{m}_s(x, y)] \quad (7)$$

Finally, we set a  $4 \times 4$  fixed filter size  $(2e+1)(2f+1)$  based from multiple observations and experimentations. Fig. 4 demonstrates excerpts of enhanced image version used for model training, with highly noticeable improvements in structural tissue details.

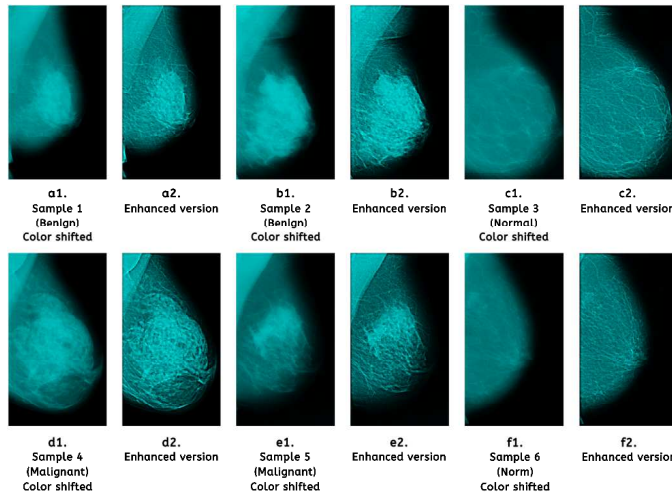


Fig. 4. Samples of color shifted (a1 to f1) and enhanced version (a2 to f2) of images with refined breast tissue details using SWF.

#### D. Residual Network with Exponential Transformations

Traditional CNNs have advanced computer vision since they are designed for discerning photographic features and patterns. At present, more than the classical approach is needed for complex classification tasks such as BC identification. First, it has a narrow receptive field, which hinders grasping an image's long-range (global context) dependencies, resulting in poor performance in attempting to understand more prominent spatial relationships. Second, its training process is plagued by complications such as vanishing or exploding gradients, which limits their capacity to learn intricacies or lack of explicit reasoning. Finally, increasing the capacity of standard CNNs by adding more layers and filters causes overfitting and increases computational power demands. Our attention-aware with fusion classifier network's backbone is a *ResNeXt*, proven highly effective for allowing diversified and fine-grained feature learning. *ResNeXt* is related to *ResNet*, the difference is the addition of 'cardinality' module (set of transformation sizes). The original *ResNet* (Fig. 5(a)) introduces shortcuts from previous to the next layer. At the same time, *ResNeXt* (Fig. 5(b)) has a parallel stacking principle with shared width and filter sizes leading to fewer hyperparameters. This mechanism facilitates information flow on various channels, making it computationally efficient. It can also be trained and deployed with better performance than its predecessors. Furthermore, adaptation to different domains is effortless through customizing the block numbers leading to

enhanced generalization. Thus, we designed a sophisticated deep learning attention-aware architecture to bolster classification with fused recurrent neural networks (RNN).

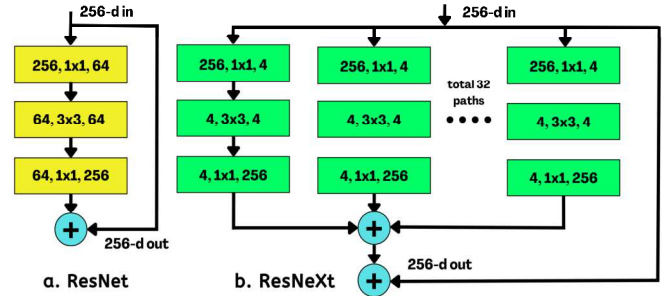


Fig. 5. ResNet (a) and ResNeXt (b) with 32 same topology or cardinality.

#### E. Proposed Attention-Aware with Fusion Classifier Network (AWFCNET)

Attention DL frameworks extract informative features by concentrating on the most salient regions of an image. This strategy is fundamental in complex image analysis, such as medical diagnoses with prevalent noise and overlapping elements. Moreover, it simplifies the model's decision to comprehend and validate. The complete pipeline's block diagram is presented in Fig. 6. Primarily, our AWFCNET's core is *ResNeXt-101* pre-trained with *ImageNet* for transfer learning [35] and a Bayes search optimized CNN with a modified attention-aware module. Its integration is sandwiched by the multiplication and rectified learning unit (ReLU) layers, with average and max pooling to create multiple feature maps (FM) sets. Next, the convolution layer combined the supplied concatenated FMs with a ReLU activation function. We customized the 'fully connected' layers with 256 nodes for the feature layer and the output dimension to 3 for three classifications (benign, malignant & normal). Although RNNs are extensively utilized for sequence modeling tasks, it is proven when combined with the strengths of a CNN.

In hybrid architecture, the two networks are well-suited on complex pattern analysis seizing the image's spatial and temporal properties. Our fused configuration employed the top three performing RNNs on shallow (3-layered) configuration based on our quantified probe such as echo state network (ESN), gated recurrent unit (GRU), and stacked bidirectional long short-term memory (S-BLSTM). S-BLSTM consists of stacked bidirectional LSTMs by processing the learned information from previous layers allowing higher level abstracted representation of the input data by learning in forward and backward directions. Compared to LSTMs, GRUs are simpler and faster to train that can address the vanishing gradient problems that makes it difficult for the network to learn from earlier known sequences. By selectively forgetting and remembering information, it can also determine the input's long-term dependencies. Lastly, ESNs have shown its versatility on large datasets with various types and dimension and remains a relative algorithm in the future. Predictions received from classifiers are combined for the final classification through hard voting.

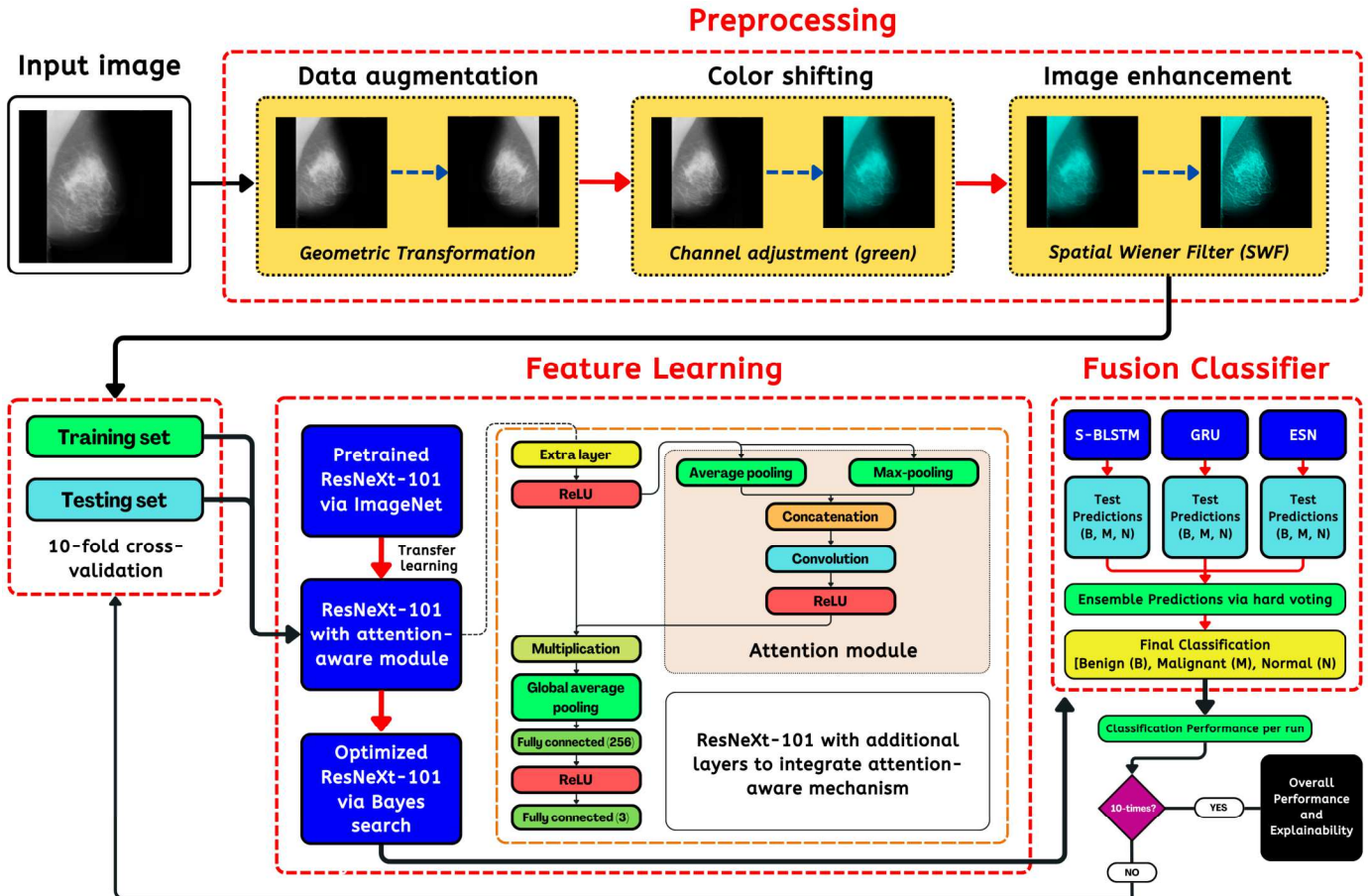


Fig. 6. AWFCNET’s block diagram for breast cancer classification (preprocessing, training & testing, feature learning, and fused RNN classifiers).

#### F. Image Enhancement Metrics

Human sensory inspection can observe improvements. Nevertheless, we opted for visual information fidelity (VIF) [36] to measure the perceived digital quality of our image enhancement process. The algorithm segments the original and processed picture into small overlapping blocks by comparing the contrast, sharpness, noise, and artifact suppression into a single score to denote the overall quality. A higher VIF score indicates better quality using correlation coefficient (CC) and Spearman rank order CC (SROCC). Experts consider 0.9 to 1 as acceptable values for medical image diagnosis. Its general equation is described below:

$$VIF = \frac{\sum_{j \in \text{subband}} I(\bar{C}^{N,j}; \bar{F}^{N,j} | S^{N,j} = s^{N,j})}{\sum_{j \in \text{subband}} I(\bar{C}^{N,j}; \bar{E}^{N,j} | S^{N,j} = s^{N,j})} \quad (8)$$

where N are blocks in j subband decomposed by  $\bar{C}^{N,j}$  with others as similarity variables.

#### G. Classification Performance Metrics

In terms of evaluation, we applied standard metrics such as F1-score, precision, recall, and accuracy based on true & false positives (TP, FP), and true & false negatives (TN, FN) summarized in Equations 9 to 12.

$$F1 - Score (FS) = 2 * \frac{Precision * Recall}{Precision + Recall} \quad (9)$$

$$Precision (PR) = \frac{TP}{TP + FP} \quad (10)$$

$$Recall (RE) = \frac{TP}{TP + FN} \quad (11)$$

$$Accuracy (AC) = \frac{TP + TN}{TP + TN + FP + FN} \quad (12)$$

#### H. Visual Interpretability

CNNs had shown impressive results in computer vision applications. However, they were portrayed as a ‘black box’ whose inner workings were difficult to comprehend regarding classification explainability. As a solution, the gradient-weighted class activation mapping (GRAD-CAM) [37] algorithm highlights the image’s most relevant regions. It uses gradients to generate feature heat maps, gain insights into how a model arrived at its prediction, and demystify its abstract nature. For this study, we utilized GRAD-CAM++ [38], an extended version of the latter that helps capture fine-grained details with generated visual explanations.

### III. RESULTS

Our AWFCNET was constructed using *Python* language and various DL libraries (*Tensorflow*, *PyTorch* & *Keras*) on a high-end computer with a Core-i7 microprocessor, 64 GB RAM, and a dedicated RTX3090Ti graphics unit. The models

can also be implemented using similar or higher specifications.

#### A. Hyperparameter Fine-Tuning

Assigning proper hyperparameters is essential because they determine how the model learns from data. Unlike learned parameters, they are set before training, directly influencing the machine's learning outcome. Using Bayes search, we configured a learning rate of 0.001, an ADAM optimizer for our CNN, 100 epochs for stability, and a mini-batch size of 64. Our S-BLSTM contains two bidirectional and one unidirectional LSTM. Identical 800 hidden and 256 feature space dimensions were set for all RNNs (Table I).

TABLE I. AWFCNET'S OPTIMIZED HYPERPARAMETERS

Hyperparameter	Configuration
Optimizer	ADAM
Learning rate	0.001
Epoch	100
Mini-batch size	64
Loss	Multiclass cross-entropy
Hidden neurons (RNNs)	800
Feature space dimension	256

#### B. Image Enhancement Performance

We tested 75 randomly picked images (25 for each group) to measure the quality improvements. Table II shows that raw input images preprocessed with color shifting and SWF bear remarkable mean results on selected data using CC and SROCC, with values of 0.961 (highly similar) and 0.958 (positive monotonic relationship). The values exhibit mammogram detailed refinement while keeping the original breast tissue structure as observed in Fig. 4.

TABLE II. IMAGE ENHANCEMENT MEAN QUALITY INDEX (N = 75)

Method	CC	SROCC
VIF	0.961	0.958

#### C. Overall Classification Performances

Table III summarizes each evaluation criterion based on 10-fold cross-validation on 249 tests data. Our framework achieved 0.981 (accuracy), 0.980 (f1-score), 0.979 (precision), and 0.981 (recall), where most values of AC and FS fall between 0.97 to 0.98 per fold implying excellent classification results.

TABLE III. AWFCNET'S CLASSIFICATION PERFORMANCE (10-FOLD)

Fold	Accuracy	F1-Score	Precision	Recall
1	0.975	0.964	0.963	0.961
2	0.978	0.977	0.977	0.978
3	0.975	0.975	0.975	0.975
4	0.981	0.981	0.982	0.981
5	0.983	0.983	0.984	0.983
6	0.987	0.987	0.988	0.987
7	0.983	0.968	0.954	0.983
8	0.987	0.988	0.988	0.988
9	0.983	0.984	0.986	0.983
10	0.982	0.989	0.989	0.989
<b>Mean</b>	<b>0.981</b>	<b>0.980</b>	<b>0.979</b>	<b>0.981</b>

#### D. Influence of Spatial Wiener Filter (SWF) and Attention-Aware Mechanism (A-ACNN) on Pipeline's Performance

We also investigated the inclusion effects of SWF and the A-ACNN mechanism on our DL pipeline. Table IV and Fig. 7 clearly showed significant impacts on classification rate by integrating both functionalities with 98.10% accuracy over the absence of one or both with 88.40%, 91.20%, and 94.80%.

TABLE IV. COMPARATIVE PERFORMANCE ON THE ABSENCE OR PRESENCE OF SPECIFIC MECHANISMS ON AWFCNET (10-FOLD)

Mechanism	Accuracy	F1-Score	Precision	Recall
No SWF & No A-ACNN	0.884	0.881	0.881	0.878
No SWF & with A-ACNN	0.912	0.905	0.889	0.917
With SWF & No A-ACNN	0.948	0.949	0.946	0.948
<b>With SWF &amp; with A-ACNN</b>	<b>0.981</b>	<b>0.980</b>	<b>0.979</b>	<b>0.981</b>

#### INFLUENCE OF DIFFERENT MECHANISMS TO THE PIPELINE'S CLASSIFICATION ACCURACY

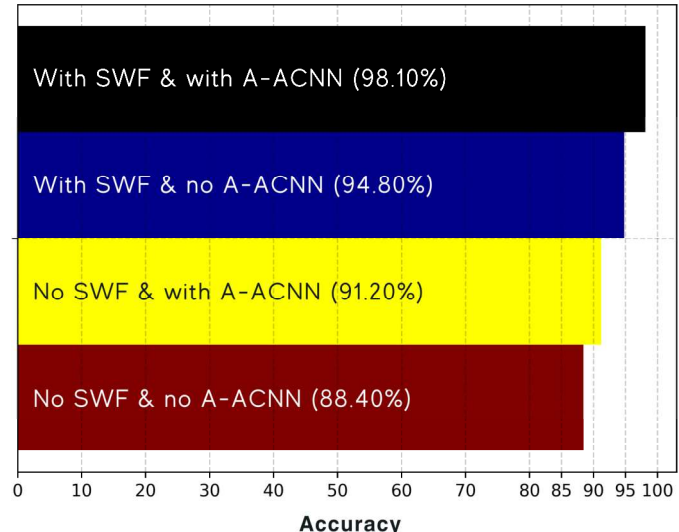


Fig. 7. Classification accuracy benchmarks demonstrating the profound effects of each mechanisms to the deep learning architecture.

#### E. Fusion Versus Individual Classifier Performance

Table V and Fig. 8 confirmed that the fusion classifiers (98.10%) outperform singular models of GRU, ESN, and S-BLSTM with 93.10%, 93.90%, and 96.80% accuracies, respectively. The ensemble also surpassed individual implementations of RNNs on related metrics with 98.00% (f1-score), 97.90% (precision), and 98.10% (recall).

TABLE V. COMPARATIVE PERFORMANCE OF INDIVIDUAL AND FUSION CLASSIFIERS ON AWFCNET, WITH SWF & WITH A-ACNN (10-FOLD)

RNN Classifier	Accuracy	F1-Score	Precision	Recall
GRU <sub>1</sub>	0.931	0.929	0.923	0.932
ESN <sub>2</sub>	0.939	0.938	0.936	0.937
S-BLSTM <sub>3</sub>	0.968	0.967	0.968	0.963
<b>Fusion<sub>(1,2,3,4)</sub></b>	<b>0.981</b>	<b>0.980</b>	<b>0.979</b>	<b>0.981</b>

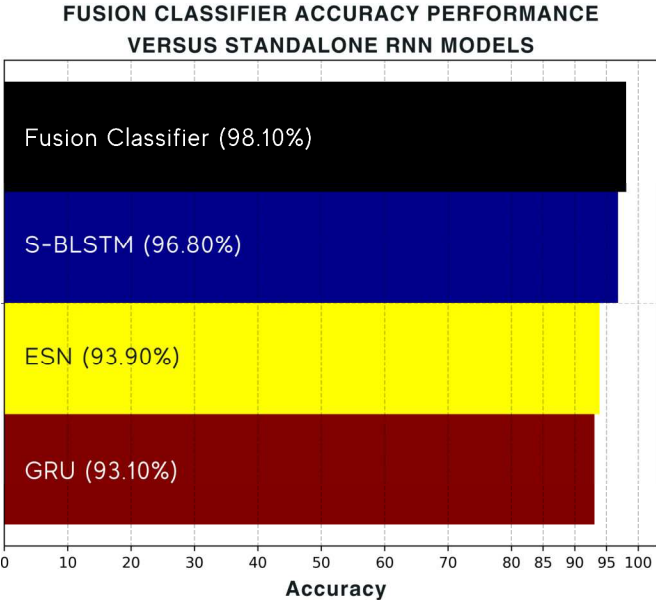


Fig. 8. Classification accuracy benchmark improvements of fusion classifier againsts individual RNN models.

#### F. Model Convergence Testing

Figure 9(a) displays a decreasing yet stabilized inter-linkage of the validation and training loss at the tail-end of the training process (75<sup>th</sup> epoch). Meanwhile, training and validation accuracy increased over time on the adjacent plot (Fig. 9(b)). It converged at the 80th epoch, with a 92 to 96 percent value range. The graphs disclosed that our proposed DL architecture showed no signs of overfitting or underfitting.

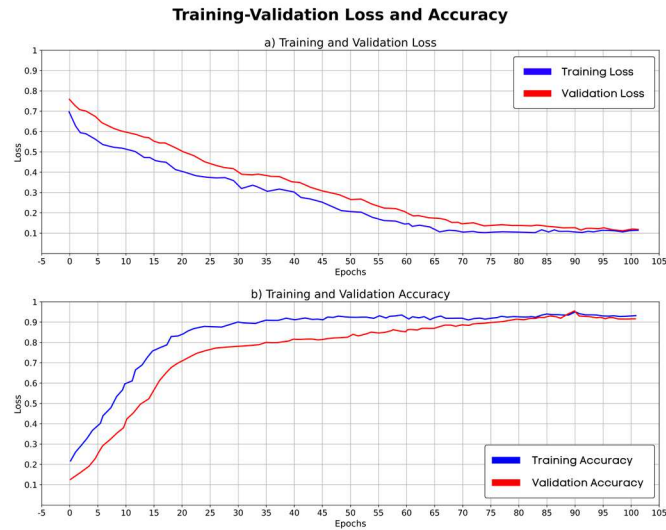


Fig. 9. The graphs demonstrated convergences conveying the lowest probability of overfitting and underfitting.

#### G. Visual Explainability

Fig. 10 presents excerpts of the GRAD CAM++ heat maps produced by AWFCNET. The red and orange (warmer colors) regions have higher activation values (ACV) corresponding to the image's most significant areas influencing the CNN's prediction. On the other hand, yellow, green, and blue (lighter colors) have lower ACV.

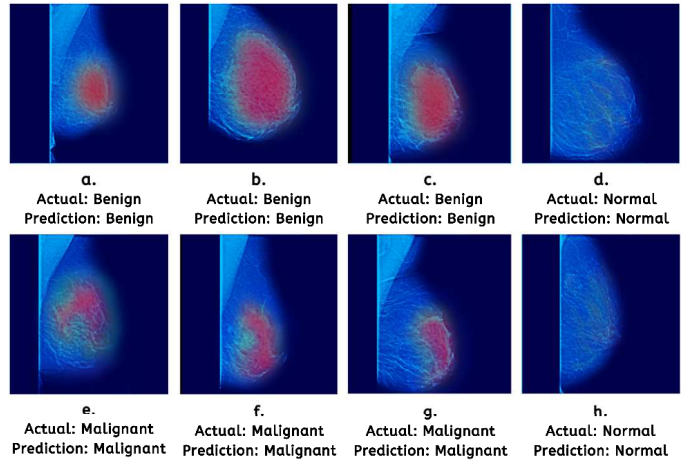


Fig. 10. Excerpts of GRAD CAM++ heatmaps based from our model.

#### H. Benchmarks with Existing Methods

We compared our approach to existing state-of-the-art techniques (architectures, preprocessing & other methods) and the quantitative results showed significant improvements in terms of accuracy (98.10%).

TABLE VI. COMPARISON WITH EXISTING DEEP LEARNING-BASED BREAST CANCER CLASSIFICATION MODELS

Models/Architectures/Approaches/Mechanisms	Accuracy
CNN + US-ELM [16]	0.865
VGG-16 + Transfer learning [21]	0.940
Modified AlexNet [22]	0.957
Lightweight CNN [23]	0.836
ELM [24]	0.960
CNN + Feature wise preprocessing [27]	0.905
CNN + Parasitic metrics layers [28]	0.967
Mixture Ensemble CNN [29]	0.963
CNN + Marine predators algorithm [30]	0.983
Multi-DCNNs [31]	0.974
Multi-DCNNs + PCA [33]	0.979
Modified CNN + Texture feature approach [34]	0.978
<b>SWF image enhancement + transfer learning + attention-aware CNN + fusion RNN classifiers (AWFCNET, our model)</b>	<b>0.981</b>

## IV. DISCUSSIONS

This study presented a comprehensive DL architecture with multiple preprocessing and special mechanisms. Experimental results ascertained that our framework outperforms traditional and existing methods for BC sub-type identification. It achieved 98.10% (accuracy), 98.00% (f1-score), 97.90% (precision), and 98.10% (recall) – indicating robustness and efficacy. Numerous factors contributed to this positive outcome. First, the color shifting and SWF preprocessing techniques increased the image's visual clarity without changing the overall structural characteristics of the raw mammogram based on VIF scores, highlighting important tissue features that were obscured beforehand. Second, the selected core of *ResNeXt-101* with cardinality module and transfer learning (pre-trained on *ImageNet*) overcame the challenges in extracting the minuscule morphological heterogeneity of tumors. Third, adding an attention-aware

module in our neural network further reinforced feature learning by concentrating on subtle yet granular tissue differences, indicative of non-cancerous and cancerous characteristics. Fourth, the inception of the fused RNN classifier at the end of the pipeline complemented the spatial learning capabilities of our modified CNN by adding the ability to recognize critical temporal dependencies in data. With the deep stacks of modules and components, the pipeline's average training time was 326 seconds.

Our investigation also underscored the importance of hyperparameter optimization to streamline the architecture's learning rate and balanced highly augmented datasets to increase training samples, which is crucial for prediction generalization. These adjustments were evident in the training/validation accuracy and loss plots that exhibited increasing gradual convergence. Lastly, we incorporated GRAD-CAM++ for visual interpretability to pervasively understand the classification decision-making of our model by zeroing in on regions of interest, including patterns. It reflected consistencies for the description of benign (round and well-defined lump) and malignant (irregular shape lump) tumors that can be potential areas for consideration by medical experts in understanding the abnormalities. We made significant advancements in AI-based medical image prognoses that are on equal ground with the work of [39 – 41].

Despite the encouraging results, our study has certain limitations. Our research evaluated and analyzed limited datasets. We cannot make a broader claim about its usefulness in other domains as it may not represent the general population considering ethnicity, race, socioeconomic background, and related variables, which can lead to biases.

## V. CONCLUSIONS AND FUTURE WORKS

Cancer is a debilitating illness affecting millions globally and remains the most pressing public health concern of our time, claiming millions of lives despite progressions in treatments. As we look ahead, it is clear that continuous research and innovation are essential to combat the disease. To elevate its diagnoses, we constructed AWFCNET, a machine learning model with extensive preprocessing (data augmentation, color shifting & image enhancement), feature extraction (transfer learning & attention-aware CNN based on *ResNeXt-101*), and ensemble RNNs for classification of BC. Our extensive experiments revealed its exceptional accuracy rate in pinpointing its sub-types compared with state-of-the-art approaches. In addition, the study disclosed explainability and interpretability through gradient mapping that can foster trust, adoption, and validation among doctors. The empirical findings from this article herald AI's revolutionary impact on healthcare systems.

We contributed to the body of science by determining the characteristics of BC using the vast tools of modern data science. It should be noted that combination of human expertise and machine learning could significantly lower diagnostic errors even in the early stages of breast cancer when it is still easily treatable. This can assist clinical practitioners and radiologists in making quick and dependable

decisions regarding patients' precise treatment plans, which could save their lives. For future work, the proponents will explore generative adversarial networks and transformers to further develop the model.

## REFERENCES

- [1] World Health Organization Newsroom, "Breast Cancer", Available at: <https://www.who.int/news-room/fact-sheets/detail/breast-cancer/>, 2021.
- [2] R. Maaliw, Z. Mabunga, M. R. de Veluz, A. Alon, A. Lagman, M. Garcia, L. Lacatan and R. Delloso, "An enhanced segmentation and deep learning architecture for early diabetic retinopathy detection," IEEE 13th Annual Ubiquitous Computing, Electronics and Mobile Communication Conference (CCWC), 2023.
- [3] R. Maaliw, A. Alon, A. Lagman, M. Garcia, J. Susa, R. Reyes, M. Fernando-Raguro and Alexander Hernandez, "A multi-stage transfer learning approach for acute lymphoblastic leukemia classification," IEEE 13th Annual Ubiquitous Computing, Electronics & Mobile Communication Conference (UEMCON), 2022.
- [4] R. Rouhi, M. Jafari, S. Kasei and P. Keshavarzian, "Benign and malignant breast tumors classification based on region growing and CNN segmentation," Expert Sys Appl, 42, pp. 990-1002, 2015.
- [5] M. Amrane, S. Oukid, I. Gagaoua and T. Ensari, "Breast cancer classification using machine learning," Electric Electronics, Computer Science, Biomedical Engineering's Meeting (EBBT), 2018.
- [6] M. Aslan, M. Unlersen, K. Sabanci and A. Durdu, "CNN-based transfer learning-BiLSTM network: A novel approach for COVID-19 infection detection," Appl Soft Comput, 98:106912, 2021.
- [7] B. Dai, R. Chen, S. Zhu and W. Zhang, "Using random forest algorithm for breast cancer diagnosis," International Symposium Computer, Consumer and Control (IS3C), pp. 449-452, 2018.
- [8] UCI Machine Learning Repository, "Breast cancer Wisconsin (diagnostic) data set", Available at: [https://archive.ics.uci.edu/ml/datasets/breast+cancer+wisconsin+\(diagnostic\)](https://archive.ics.uci.edu/ml/datasets/breast+cancer+wisconsin+(diagnostic)), 2023.
- [9] A. Ghasemzadeh, S. Azad and E. Esmaeili, "Breast cancer detection based on Gabor-wavelet transform and machine learning methods," Int. J. Mach. Learn. Cybern. 10(7), pp. 1603-1612, 2018.
- [10] J. Suckling, J. Parker, D. Dance, S. Astley, I. Hutt, C. Boggis, I. Ricketts et al., "Mammographic Image Analysis (MIAS) database v.1.21," Available at: <https://www.repository.cam.ac.uk/handle/1810/250394/>, 2015.
- [11] M. Gupta and B. Gupta, "A comparative study of breast cancer diagnosis using supervised learning techniques," Proceedings of the Second International Conference on Computing Methodologies and Communication (ICCMC), 2018.
- [12] M. Heidari, A. Khuzani, A. Hollingsworth, G. Danala, S. Mirniaharikandehei, Y. Qiu, H. Liu and B. Zheng, "Prediction of breast cancer risk using a machine learning approach embedded with a locality preserving projection algorithm," Phys. Med. Biol., 63(3), 035020, 2018.
- [13] L. Hussain, W. Aziz, S. Saeed, S. Rathmore and M. Rafique, "Automated breast cancer detection using machine learning techniques by extracting different feature extracting strategies," IEEE 17<sup>th</sup> International Conference on Trust, Security and Privacy in Computing and Communications/12<sup>th</sup> IEEE International Conference on Big Data Science and Engineering (TrustCom/BigDataSE), pp. 327-331, 2018.
- [14] A. Setiawan, J. Wesley and Y. Purnama, "Mammogram classification using law's texture energy measure and neural networks," Neurocomputing, 173, pp. 930-941, 2016.
- [15] F. Gao, T. Wu, J. Li, B. Zheng, L. Ruan, D. Shang and B. Patel, "SD-CNN: A shallow-deep CNN for improved breast cancer diagnosis," Comput. Med. Imag. Graph, 70, pp. 53-62, 2018.
- [16] D. Wang, A. Khosla, R. Gargyaya, H. Irshad and A. Beck, "Deep learning for identifying metastatic breast cancer", arXiv preprint, 2016.

- [17] D. Singh, S. Singh, M. Sonawane, R. Batham and P. Satpute, "Breast cancer detection using convolution neural network," *Int. Res. J. Eng. Technol.*, 5(6), pp. 316-318, 2018.
- [18] F. Spanhol, L. Oliveira, P. Cavalin, C. Petitjean and L. Heutte, "Deep features for breast cancer histopathological image classification," *IEEE International Conference on Systems, Man, and Cybernetics (SMC)*, pp. 1868-1873, 2018.
- [19] H. Chen, Q. Dou, X. Wang, J. Qin and P. Heng, "Mitosis detection in breast cancer histology images via deep cascaded networks," *Proceedings of the AAAI Conference on Artificial Intelligence*, 30(1), 2016.
- [20] R. Mokni and M. Haoues, "CADNet157 model: Fine-tuned ResNet152 model for breast cancer diagnosis from mammography images," *Neural Computing and Applications*, pp. 1-24, 2022.
- [21] N. Ismail and C. Sovuthy, "Breast cancer detection based on deep learning technique," *IEEE International UNIMAS STEM 12<sup>th</sup> Engineering Conference (EnCon)*, pp. 89-94, 2019.
- [22] E. Omonigho, M. David, A. Adejo and S. Aliyu, "Breast cancer: Tumor detection in mammogram images using modified AlexNet deep convolution neural network," *IEEE International Conference in Mathematics, Computer Engineering and Computer Science (ICMCECS)*, pp. 1-6, 2020.
- [23] P. Shi, C. Wu, J. Zhong and H. Wang, "Deep learning from small dataset for BI-RADS density classification of mammography images," *IEEE 10<sup>th</sup> International Conference on Information Technology in Medicine and Education (ITME)*, pp. 102-109, 2019.
- [24] W. Xie, Y. Li and Y. Ma, "Breast cancer classification using law's texture energy measure and neural networks," *Procedia Comput Sci*, 59, pp. 92-97, 2018.
- [25] Z. Wang, M. Li, H. Wang, H. Jiang, Y. Yao and H. Zhang et al., "Breast cancer detection using extreme learning machine based on feature fusion with CNN deep features," *IEEE Access*, 7, 105146-58, 2019.
- [26] R. Patil and N. Biradar, "Automated mammogram breast cancer detection using the optimized combination of convolutional and recurrent neural network," *Evol Intell*, pp. 1-16, 2020.
- [27] F. Ting, Y. Tan and K. Sim, "Convolutional neural network improvement for breast cancer classification," *Expert Syst Appl*, 120, pp. 103-115, 2019.
- [28] Z. Jiao, X. Gao, Y. Wang and J. Li, "A parasitic metring learning net for breast mass classification based on mammography," *Pattern Recognition*, 75, pp. 292-301, 2018.
- [29] R. Rasti, M. Teshnehab and S. Phung, "Breast cancer diagnosis in DCE-MRI using mixture ensemble of convolutional neural network," *Pattern Recognition*, 72, pp. 381-390, 2018.
- [30] E. Houssein, M. Emam and A. Ali, "An optimized deep learning architecture for breast cancer diagnosis based on improved marine predators algorithm," *Neural Comput Appl*, 2022.
- [31] D. Ragab, O. Attallah, M. Sharkas, J. Ren and S. Marshall, "A framework for breast cancer classification using multi-DCNNs," *Comput Biol Med*, 131, 104245, 2021.
- [32] W. Salama and M. Aly, "Deep learning in mammography images segmentation and classification: Automated CNN approach," *Alexandria Eng J*, 60, pp. 4701-4709, 2021.
- [33] S. Chakravarthy, N. Bharanidharan and H. Rajaguru, "Multi-deep CNN based experimentations for early diagnosis of breast cancer," *IETE J Res*, pp. 1-16, 2022.
- [34] J. Melekooodappattu, A. Dhas, B. Kandathil and K. Adarsh, "Breast cancer detection in mammogram: Combining modified CNN and texture feature based approach," *J Ambient Intell Hum Comput*, 2022.
- [35] R. Maaliw, A. Alon, A. Lagman, M. Garcia, M. Abante, R. Belleza, J. Tan and R. Maaño, "Cataract detection and grading using ensemble neural networks and transfer learning," *IEEE 13<sup>th</sup> Annual Information Technology, Electronics and Mobile Communication Conference (IEMCON)*, pp. 74-81, 2022.
- [36] C. Peng, M. Wu and K. Liu, "Multiple levels perceptual noise backed visual information fidelity for picture quality assessment," *IEEE International Symposium on Intelligent Signal Processing and Communication Systems (ISPACS)*, pp. 1-4, 2022.
- [37] V. Jahmunah, E. Ng, R. Tan, S. Oh and U. Acharya, "Explainable detection of myocardial infarction using deep learning models with Grad-CAM technique on ECG signals," *Computers in Biology and Medicine*, 146, 105550, 2022.
- [38] X. Inbaraj, C. Villavicencio, J. Macrohon, J. Jeng and J. Hsieh, "Object identification and localization using Grad-CAM++ with mask regional convolution neural network," *Electronics*, 10(13), 1541, 2021.
- [39] M. Soni, A. Singh, B. Suresh and Sumit Kumar, "Convolutional neural network based CT scan classification method for COVID-19 test validation," *Smart Health*, 25, 100296, 2022.
- [40] I. Keshta, S. Pallavi, M. Shabaz, M. Soni, M. Bhadla and Y. Muhammed, "Multi-stage biomedical feature selection extraction algorithm for cancer detection," *SN Applied Sciences*, 5, 2023.
- [41] R. Maaliw, J. Susa, A. Alon, A. Lagman, S. Ambat, M. Garcia, K. Piad and M. Fernando-Raguro, "A deep learning approach for automatic scoliosis cobb angle identification," *IEEE World Artificial Intelligence & Internet of Things Congress (AIIoT)*, 2022.

All



ADVANCED SEARCH

Conferences > 2023 IEEE World AI IoT Congre... ?

# AWFCNET: An Attention-Aware Deep Learning Network with Fusion Classifier for Breast Cancer Classification Using Enhanced Mammograms

Publisher: IEEE

Cite This

PDF

Renato R. Maaliw ; Mukesh Soni ; Manuel P. Delos Santos ; Maria Rossana D. de Veluz ; ... All Authors



Request permission for reuse.

## Abstract

### Abstract:

Breast cancer remains a significant public health concern and a leading cause of female mortality despite recent advances in healthcare. Experts agree that its early prognosis is a key to survivability. In this research, we proposed a deep learning architecture code-named AWFCNET. It comprised multiple segments of preprocessing techniques (color shifting & image enhancement), feature learning based on ResNeXt-101 convolutional network as a backbone with transfer and attention-aware mechanisms, and fusion classifier composed of three recurrent neural networks. The generalization capability of the pipeline produced 98.10% accuracy on a mammogram dataset using 10-fold cross-validation. Computational benchmarks revealed that it surpassed existing state-of-the-art approaches with provisions of visual interpretability via gradient maps. Thus, our framework could complement physicians' expertise in rapid and dependable breast cancer diagnoses.

## Authors

Published in: 2023 IEEE World AI IoT Congress (AlloT)

## Figures

## References

Date of Conference: 07-10 June 2023

DOI:

10.1109/AlloT58121.2023.10174427

## Keywords

Date Added to IEEE Xplore: 13 July 2023

Publisher: IEEE

### ISBN Information:

Electronic ISBN: 979-8-3503-3761-7

Print on Demand(PoD)

ISBN: 979-8-3503-3762-4

Conference Location: Seattle, WA, USA

## I. Introduction

Breast cancer (BC) is a lethal disease caused by the immediate mutation of internal nucleolus cells in the breast. Recent statistical figure reports its prevalence in women, accounting for 26% of all cancer cases. In 2021, an estimated 2.5 million instances and 630,000 deaths transpired worldwide [1]. According to specialists, these mortality rates can be reduced by 80% through early detection,

Need  
Full-Text

access to IEEE Xplore  
for your organization?

CONTACT IEEE TO SUBSCRIBE >

## More Like This

Low-Complexity Nonlinear  
Adaptive Filter Based on a  
Pipelined Bilinear Recurrent  
Neural Network

IEEE Transactions on Neural Networks  
Published: 2011

Predictive Modeling of Therapy  
Decisions in Metastatic Breast  
Cancer with Recurrent Neural  
Network Encoder and Multinomial  
Hierarchical Regression Decoder

2017 IEEE International Conference on  
Healthcare Informatics (ICHI)  
Published: 2017

Show More



where they are still easily treatable. Mammography, ultrasound, magnetic resonance imaging (MRI), histopathology, and thermography are widely used to produce clear pictures of internal organs for medical diagnosis. Despite these innovations, manually interpreting these images can be time-consuming, stressful, and inconsistent [2]. Comparing benign (non-aggressive) and malignant (aggressive) tumors are complex, as the difference between dense and cancerous tissue is challenging to comprehend (Fig. 1). Integration of state-of-the-art technology with established practices is paramount to improving prognosis. The advent of artificial intelligence (AI) has marked a significant advancement in computer-assisted

[Sign in to Continue Reading](#)



## Authors

### Renato R. Maaliw

College of Engineering, Southern Luzon State University, Lucban, Quezon, Philippines

### Mukesh Soni

Department of CSE, Chandigarh University, Mohali, Punjab, India

### Manuel P. Delos Santos

College of Allied Medicine, Southern Luzon State University, Lucban, Quezon, Philippines

### Maria Rossana D. de Veluz

College of Engineering, Southern Luzon State University, Lucban, Quezon, Philippines

### Pitz Gerald G. Lagazon

College of Engineering, Southern Luzon State University, Lucban, Quezon, Philippines

### Mariebeth P. Seño

College of Arts & Sciences, Southern Luzon State University, Lucban, Quezon, Philippines

### Devie R. Salvatierra - Bello

College of Industrial Technology, Southern Luzon State University, Lucban, Quezon, Philippines

### Reynaldo V. Danganan

College of Industrial Technology, Southern Luzon State University, Lucban, Quezon, Philippines

## Figures



## References



## Keywords



## IEEE Personal Account

CHANGE  
USERNAME/PASSWORD

## Purchase Details

PAYMENT OPTIONS  
VIEW PURCHASED  
DOCUMENTS

## Profile Information

COMMUNICATIONS  
PREFERENCES  
PROFESSION AND EDUCATION  
TECHNICAL INTERESTS

## Need Help?

US & CANADA: +1 800 678  
4333  
WORLDWIDE: +1 732 981  
0060

## Follow

[CONTACT & SUPPORT](#)

# What are the Benefits of Publishing with IEEE?

## Discoverability

### Ensure That Your Work is Found

With its robust search features, researchers trust the IEEE *Xplore*® digital library to find what they need, saving time and maximizing results.

### Authors Benefit from Strong IEEE *Xplore* Usage

Eight million downloads per month by more than three million users is strong evidence that IEEE *Xplore* provides authors with the exposure they seek.

### Our Partners Help You

Access to author content is increased by the relationships IEEE has with referencing, indexing, and abstracting providers. IEEE content is indexed and discoverable in Inspec, Ei Compendex, Scopus®, Clarivate Analytics WoS, EBSCOhost, and Google Scholar, among others.

## Credibility

### Longevity = Trust

IEEE has maintained a brand and reputation as a trusted source of cutting-edge research for more than 125 years.

### Peer Review

The IEEE commitment to peer review ensures the high quality of every article accepted.

### Top Ranked Journals

Year after year, IEEE journals are top ranked in the Thomson Reuters Journal Citation Reports® (JCR), with established impact factors among the highest in the field.

## Opportunity

### IEEE Authors are Active

Over 1,000 articles are added daily to the more than four million documents in IEEE *Xplore*.

### Convenient Author Tools

Resources are available to help manage the workflow, from manuscript development through the publishing process, and to help connect with leading voices in technology.

### Wide Range of Publications

With approximately 200 journals and magazines and more than 1,500 conferences, authors can select from a wide variety of titles in electrical engineering and computing.

### Open Access Options

To help authors gain maximum exposure for their articles, IEEE offers three open access (OA) publishing options: a multidisciplinary open access journal, hybrid journals, and fully open access topical journals—all designed to meet the varying needs of our authors.

## Flexibility

### Streamlined Publishing

Authors can optimize the publishing process with a web-based workflow, electronic submission via ScholarOne Manuscripts, and tracking of an article's progress.

### Efficient Timeline

IEEE publishes articles, not issues, so there is no additional wait for an entire journal issue to be assembled.

### Author Support

Authors, from beginners to previously published, will find the assistance they need during all phases of manuscript development, submission, and publication.



**CREDIBLE:**  
IEEE publishes many of the top electrical and electronic engineering titles.

Source: Thomson Reuters Journal Citation Reports.



**FINDABLE:**  
Researchers trust IEEE—8 million downloads per month from the IEEE *Xplore* digital library.



**FLEXIBLE:**  
Publishing options from traditional journals to open access.



#115 (1570906076): AWFCNET: An Attention-Aware Deep Learning Network With Fusion Classifier for Breast Cancer Classification Using Enhanced Mammograms

## #115 (1570906076): AWFCNET: An Attention-Aware Deep Learning Network With Fusion Classifier for Breast Cancer Classification Using Enhanced Mammograms

[Hide details](#)

BIBTeX

**Authors** Renato R. Maaliw III (Southern Luzon State University, Philippines); Mukesh Soni (Chandigarh University, India); Manuel P. Delos Santos, Maria Rossana D. De Veluz, Pitz Gerald G. Lagazon, Mariebeth P. Seño, Devie R. Salvatierra - Bello and Reynaldo V. Danganan (Southern Luzon State University, Philippines)



**Paper title** AWFCNET: An Attention-Aware Deep Learning Network With Fusion Classifier for Breast Cancer Classification Using Enhanced Mammograms Only the chairs can edit

**Conference and track** 2023 IEEE World AI IoT Congress (AlloT) - 2023 IEEE World AI IoT Congress (AlloT) Regular Research Paper

**Abstract**  Only the chairs can edit Breast cancer remains a significant public health concern and a leading cause of female mortality...

**Keywords** ensemble prediction; hybrid model; image enhancement; medical diagnosis; ResNeXt-101; tumors Only the chairs can edit

**Topics** Computer Vision and Speech Understanding; Pattern Recognition Only the chairs can edit [+](#)

**Personal notes** [+](#)

**Roles** You are the creator, an author and a presenter for this paper.  
You have authored an accepted paper in this conference.

**Status** Accepted [×](#)

**Copyright** [+](#) IEEE; IEEE: May 16, 2023 00:00 Asia/Hong\_Kong

**Registration** [✉](#) Renato R. Maaliw III has registered and paid for Tt:IEEM [×](#) [✉](#)

**Presented** by Renato R. Maaliw III (bio) [✉](#) [+](#)

**Presentation** [Final manuscript](#)



completed

## Comments

The paper should be accepted in its current form.  
However, the authors did not anonymize themselves in the paper.

completed

## Comments

- The paper proposes a deep learning architecture called AWFCNET for breast cancer classification.
- Experimental results show that the proposed approach outperforms existing methods.
- There is a need to use a larger dataset.
- Add a block diagram in section II to show the proposed method.

completed

## Comments

Authors are requested to change the title.  
The title seems too long and it is very hard to get the paper topics.  
Too many references are cited. If possible, remove some unnecessary.

# FACULTY POSITION RECLASSIFICATION FOR SUCS

(DBM-CHED Joint Circular No. 3, series of 2022)

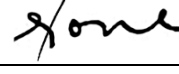
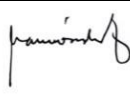
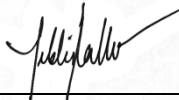
## CERTIFICATION OF PERCENTAGE CONTRIBUTION

(Research Output with Multiple Authors)

**Title of Research:** AWFCNET: An Attention-Aware Deep Learning Network with Fusion Classifier for Breast Cancer Classification Using Enhanced Mammograms

**Type of Research Output:** Conference Paper (Scopus-Indexed, IEEE Paper)

**Instruction:** Supply ALL the names of the authors involved in the publication of Research output and indicate the contribution of each author in percentage. Each author shall sign the conforme column if he/she agrees with the distribution. The conforme should be signed by all the authors in order to be considered. Please prepare separate Certification for each output.

	Name of Authors	% Contribution	Conforme (Sign if you agree with the % distribution)
1	Renato R. Maaliw III	30%	
2	Mukesh Soni	10%	
3	Manuel P. Delos Santos	10%	
4	Maria Rossana D. De Veluz	10%	
5	Pitz Gerald G. Lagazon	10%	
6	Mariebeth P. Seño	10%	
7	Devie R. Salvatierra – Bello	10%	
8	Reynaldo V. Danganan	10%	
	* Should have a total of 100%	100.00%	

Prepared by:

**Renato R. Maaliw III, DIT**  
(Name and Signature)  
Faculty

Certified by:

**Nicanor L. Guinto, Ph.D**  
(Name and Signature)  
Director, Office of Research Services